The Proximal Ligand Variant His93Tyr of Horse Heart Myoglobin†

Dean P. Hildebrand, David L. Burk, Robert Maurus, Juan C. Ferrer, Gary D. Brayer,* and A. Grant Mauk*

Department of Biochemistry and Molecular Biology and Protein Engineering Network of Centres of Excellence, University of British Columbia, Vancouver, British Columbia, V6T 1Z3 Canada

Received August 23, 1994; Revised Manuscript Received October 12, 1994®

ABSTRACT: The spectroscopic and structural properties of the His93Tyr variant of horse heart myoglobin have been studied to assess the effects of replacing the proximal His residue of this protein with a tyrosyl residue as occurs in catalases from various sources. The variant in the ferric form exhibits electronic spectra that are independent of pH between pH 7 and 10, and it exhibits changes in absorption maxima and intensity that are consistent with a five-coordinate heme iron center at the active site. The EPR spectrum of the variant is that of a high-spin, rhombic system similar to that reported for bovine liver catalase. The 1D ^{1}H-NMR spectrum of the variant confirms the five-coordinate nature of the heme iron center and exhibits a broad resonance at 112.5 ppm that is attributable to the *meta* protons of the phenolate ligand. This result indicates that the new Tyr ligand flips at a significant rate in this protein. The thermal stability of the Fe(III) derivative is unchanged from that of the wild-type protein (pH 8) while the midpoint reduction potential [−208 mV vs SHE (pH 8.0, 25 °C)] is about 250 mV lower. The three-dimensional structure of the variant determined by X-ray diffraction analysis confirms the five-coordinate nature of the heme iron center and establishes that the introduction of a proximal Tyr ligand is accommodated by a shift of the F helix (residues 88−99) in which this residue resides away from the heme pocket. Additional effects of this change are small shifts in the positions of Leu29, a heme propionate, and a heme vinyl group that are accompanied by altered hydrogen bonding interactions with the heme prosthetic group. The position of the Tyr93 residue with respect to the heme group is also different from that of the His93 residue normally present and resembles that of the proximal Tyr residue of bovine liver catalase.

Understanding the manner in which the heme binding environment provided by the apoprotein dictates the ligand binding and catalytic properties of heme proteins remains one of the fundamental objectives of research concerning this family of proteins. As one of the most significant structural characteristics of such proteins is the coordination environment of the heme iron, the application of site-directed mutagenesis to the investigation of the relatively simple heme protein myoglobin has led to the production of several variants in which the coordination of the water molecule normally bound as the sixth ligand to the heme iron has been perturbed by replacing the so-called "distal" histidine (His64) residue that normally forms a hydrogen bond with this water molecule with a variety of amino acids (e.g., Springer et al., 1994). On the other hand, the proximal His93 residue has been studied less extensively, and at present, the only variants of this type reported are the Tyr variant of sperm whale (Egeberg et al., 1990; Morikis et al., 1990) and human (Adachi et al., 1991, 1993) myoglobin and the Cys variant of human Mb (Adachi et al., 1991, 1993). The emphasis of these previous studies has been investigation of selected spectroscopic and ligand binding consequences of these substitutions, so several critical structural and functional aspects of these proteins remain to be elucidated. In terms of three-dimensional structural studies, these have thus far been restricted to consideration of variants of the distal His residue (Quillin et al., 1993; Rizzi et al., 1993; Hargrove et al., 1994; Maurus et al., 1994).

The present study defines the structural, functional, and spectroscopic consequences of replacing the proximal His ligand to the heme iron of horse heart myoglobin with a tyrosyl residue. This variant is of interest not only as a probe of myoglobin function but also because the enzyme catalase possesses a proximal tyrosyl heme iron ligand as demonstrated by X-ray crystallographic studies of catalases from mammalian (Reid et al., 1981; Murthy et al., 1981; Fita & Rossmann, 1985, 1986), fungal (Vainshtein et al., 1986), and bacterial (Murshudov et al., 1992) sources. Investigation of a myoglobin derivative with the same proximal ligand provides a means of determining the extent to which this change in ligation determines the spectroscopic, functional, and structural properties of the protein relative to the contributions made by the other, extensive differences in structures between myoglobin and catalase.

The status of the distal (or sixth) heme ligand is also of considerable interest in this variant because crystallographic characterization of catalase from bovine liver (Fita & Rossman, 1985, 1986) has demonstrated that this enzyme lacks a water molecule bound as the distal ligand while the corresponding bacterial enzyme (Murshudov et al., 1992) has a water molecule bound as the sixth ligand. It is, therefore, of interest to determine the extent to which the coordination environment of horse heart myoglobin is dictated by the residues lining the distal heme pocket and to what extent it is influenced by a *trans* effect provided by the identity of the proximal ligand. Comparison of the properties of this variant with those of catalases and naturally occurring hemoglobin variants with similar substitutions permits definition of these factors in greater detail.

† Supported by the Protein Engineering Network of Centres of Excellence. R.M. is the recipient of an MRC of Canada Studentship. The NMR spectrometer was supported by MRC Maintenance Grant ME-7826 (to Professor Pieter R. Cullis).

® Abstract published in *Advance ACS Abstracts,* January 1, 1995.

0006-2960/95/0434-1997$09.00/0

EXPERIMENTAL PROCEDURES

Site-Directed Mutagenesis and Myoglobin Expression. The construction and expression of a synthetic gene coding for wild-type horse heart myoglobin in *Escherichia coli* have been described previously (Guillemette et al., 1991). Oligonucleotide-directed mutagenesis techniques were used to construct the proximal ligand variant used in this work (Zoller & Smith, 1983, 1984). Potential mutants were screened by single-stranded DNA sequencing (Maniatis et al., 1989). Restriction enzymes were obtained from Pharmacia, and all other enzymes were obtained from Sigma.

Protein Purification. Cells from 12 L of bacterial culture were collected by centrifugation and suspended in buffer [20 mM Tris-HCl, pH 8.4 (100 mL)]. To lyse these cells, lysozyme (250 mg) was added, and the suspension was frozen in liquid nitrogen. Upon thawing, deoxyribonuclease I (10 mg), (Sigma, D5025), ribonuclease A (1 mg) (Sigma, R4875), and 20 mL of 2 M $MgCl_2$ solution were added, and the suspension was left on ice for several hours. The resulting cellular debris was removed by centrifugation (Sorvall GS-3 rotor, 8000 rpm, 30 min). The brownish supernatant fluid was brought to 55% saturation by the slow addition of solid ammonium sulfate and was then stirred on ice for 1 h. The resulting precipitate was removed by centrifugation (GS-3 rotor, 8000 rpm, 30 min), and the supernatant fluid was brought to 100% saturation with ammonium sulfate as before. The precipitated protein was dissolved in distilled water and dialyzed against water at 4 °C.

The dialyzed supernatant fluid was centrifuged (Sorvall GS-3 rotor, 8000 rpm, 30 min), adjusted to pH 8.0, and applied to a DEAE-Sepharose CL-6B (Pharmacia) column (2.5 × 10 cm) that was equilibrated with 50 mM Tris-HCl buffer (pH 8.0). Myoglobin eluted upon subsequent washing with the equilibration buffer and was applied directly to a zinc chelate affinity column that had been prepared as follows. Chelating Sepharose (2.5 × 6 cm) (Pharmacia) was charged with 700 mL of 35 mM zinc sulfate/25 mM acetic acid and equilibrated with 1 L of 5 mM Tris-HCl/0.5 M NaCl (pH 8.0). Both the apo- and holoprotein bound to the column and eluted with 50 mM Tris-HCl buffer containing 50 mM imidazole and 0.5 M NaCl (pH 8.0). The eluted protein was exchanged into a buffer containing 0.1 M potassium phosphate (dibasic), 0.1 M potassium chloride, and 10% glycerol (pH 9.0). At this stage, the myoglobin was estimated to be >90% pure by SDS−polyacrylamide gel electrophoresis.

The low level of holo-His93Tyr produced in *E. coli* eliminates any contribution of sulfmyoglobin production during expression of this variant (Lloyd & Mauk, 1994). To reconstitute the variant apoprotein, a slight excess of hemin (Sigma, H2250) dissolved in a minimum of NaOH solution (0.1 M) was added. Hemin uptake by the apoprotein was monitored by the increased intensity of the Soret band at 403 nm. Excess hemin was removed by elution of the reconstitution mixture over a Sephadex G-75 superfine (Pharmacia) column (2.5 × 90 cm) equilibrated with 50 mM Tris-HCl buffer containing 1 mM EDTA (pH 8.4). Extinction coefficients were determined by the pyridine hemochromogen method (De Duve, 1948).

Spectroscopy. Electronic absorption spectra were recorded at 25 °C with a Cary 219 spectrophotometer interfaced to a microcomputer (On-Line-Instrument-Systems, Bogart, GA) and fitted with a water-jacketed cell holder and a circulating water bath. EPR spectra were obtained at 4 K with a Bruker Model ESP 300E spectrometer (modulation frequency 100 kHz, modulation amplitude 8 G, microwave frequency 9.46 GHz, power 0.50 mW) equipped with an HP5352B microwave frequency counter and an Oxford Instruments ESR900 continuous-flow cryostat. Protein samples (1 mM) for EPR spectroscopy were prepared in 20 mM Tris-HCl/1 mM EDTA (pH 8.0).

Circular dichroism measurements were made with a Jasco Model J-720 spectropolarimeter under computer control. The temperature of the sample was regulated with a Neslab Model RTE-110 water bath that was also under computer control. Samples were prepared in 35 mM sodium phosphate (pH 8.0) with an absorbance at 280 nm of 0.6. The change in ellipticity was monitored at 222 nm over a temperature range of 45−85 °C and a temperature slope of 50 °C/h. Melting temperatures (T_m) were determined from the first derivative of the ellipticity vs temperature plot.

NMR spectra were recorded at 20 °C with a Bruker MSL-200 spectrometer operating in the quadrature mode at 200 MHz. Protein samples (2 mM) were exchanged into 50 mM deuterated sodium phosphate buffer, pH 7.0 (uncorrected pH-meter reading). Typical spectra consisted of 30−60 K transients collected over a 62.5 kHz bandwidth with 8192 data points and using a superWEFT pulse sequence (Inubushi & Becker, 1983). Before Fourier transformation, the free induction decay was apodized by an exponential function which introduced 30 Hz line broadening. Chemical shifts are referenced to DSS (2,2-dimethyl-2-silapentane-5-sulfonate) through the residual water reference.

Electrochemical Measurements. The midpoint reduction potential of this variant was determined with a photochemical titration method using riboflavin/EDTA (Mauro et al., 1988). Solutions prepared for these measurements contained 35 mM sodium phosphate, 10 mM EDTA, 21 μM riboflavin, and 15 μM protein (pH 8.0). Oxygen was excluded by the use of an anaerobic cuvette and thorough purging of the solutions with argon gas prior to protein addition. Reduction proceeded by direct illumination of the sample for increasing periods of time. Riboflavin reduction was monitored at 452 nm, and reduction of the His93Tyr variant was monitored at 598 nm. The reduction potential of riboflavin was assumed to be −233 mV vs SHE (Draper & Ingraham, 1968).

Structure Determination. Crystals of the His93Tyr variant were grown at room temperature by a combination of the hanging drop vapor diffusion method and a hair-seeding technique (Leung et al., 1989). A 5 μL droplet containing protein (15 mg/mL), 60% saturated ammonium sulfate, 20 mM Tris-HCl, and 1 mM EDTA (pH 7.7−7.9) was suspended over a well containing 1 mL of 65−66% saturated ammonium sulfate, 20 mM Tris-HCl, and 1 mM EDTA (pH 7.7−7.9). The crystals obtained were found to be isomorphous with those of both wild-type (Evans & Brayer, 1988, 1990) and recombinant wild-type (Maurus et al., 1994) horse heart myoglobin.

Diffraction data for the variant were collected to a resolution of 1.7 Å from two crystals with a Rigaku R-Axis II imaging plate area detector system. The incident radiation consisted of CuK_α X-rays from a rotating anode generator operated at 59 kV and 90 mA. Individual data collection frames were exposed for 40 min, during which time the

Table 1: Data Collection and Refinement Parameters

(I) Data Collection	
space group	$P2_1$
cell dimensions (Å)	
a	65.4
b	28.9
c	35.9
β (deg)	107.1
no. of reflections measured	29784
no. of unique reflections	11147
merging *R*-factor (%)[a]	5.7
resolution range (Å)	8.0−1.7
(II) Refinement	
no. of reflections used	9888
resolution range (Å)	5.0−1.7
data cutoff	$F > 2\sigma(F)$
no. of protein atoms	1244
no. of solvent molecules	79
average thermal factors (Å^2)	
protein atoms	19.3
solvent atoms	31.7
final refinement *R*-factor (%)[b]	15.1

[a] $R_{merge} = \sum_{hkl}\sum_{i=0}^{n}|Fi_{hkl} - \overline{F}_{hkl}|/\sum_{hkl}\sum_{i=0}^{n}Fi_{hkl}$. [b] $R_{cryst} = \sum_{hkl}|F_o - F_c|/\sum_{hkl}|F_o|$.

oscillation angle was set to 1.5° (70 frames) and 2° (80 frames) for the first and second crystals, respectively. The frame images collected were processed to structure factor amplitudes with the R-Axis II system software (Sato et al., 1992). The absolute scales of each of the two data sets for the variant were derived by linear rescale against a wild-type horse heart myoglobin data set. The two individual data sets were then merged to produce a single set of structure factors for use in refinement. A summary of data collection parameters is given in Table 1.

Least-squares restrained parameter refinement (Hendrickson & Konnert, 1981) was initiated using the structure of horse heart myoglobin (Maurus et al., 1994) as a starting model with residue 93 represented as an alanine. The initial crystallographic *R*-factor obtained was 31%, which showed little improvement over 10 cycles of refinement, suggesting that structural differences between the His93Tyr variant and wild-type proteins were substantial. To overcome this problem, the simulated annealing technique with a slow cooling protocol (X-PLOR; Brünger, 1990) was used to obtain a better fit of the starting model to the observed diffraction data. This new starting model was then used to begin a new round of conventional least-squares refinement which proceeded with a steadily improving crystallographic *R*-factor.

During refinement, periodic inspection of fragment-deleted, $F_o - F_c$, and $2F_o - F_c$ difference electron density maps allowed location of the remaining atoms of the Tyr93 side chain as well as the repositioning of the side chains of several surface residues. Water molecules were identified by an automated solvent search method (Tong et al., 1994) and manually confirmed using $2F_o - F_c$ and $F_o - F_c$ difference electron density maps. Water molecules were retained in the refinement model only if they participated in reasonable hydrogen bonds to protein atoms and had refined thermal factors of less than 55 Å^2. All water molecules were refined as oxygen atoms with full occupancy. One sulfate ion was also identified and refined with an average thermal factor of 34.6 Å^2 for the constituent atoms. The final statistics for the refinement of the His93Tyr variant structure are given in Table 1. The resulting structural model has rms deviations from ideal values for bond and angle distances of 0.18 and 0.035 Å, respectively.

Table 2: Electronic Absorption Maxima and Molar Absorptivities for Wild-Type Myoglobin and the His93Tyr Variant

	absorption maxima [nm (mM^{-1} cm^{-1})]			
protein	Soret	visible		
wild-type[a]				
Fe(III)	408 (188)	502 (10)		630 (4)
Fe(II)	435 (121)		560 (14)	
Fe(II)CO	424 (207)	540 (15)		579 (14)
His93Tyr[b]				
Fe(III)	403 (111)	487 (15)	524 (13)	599 (13)
Fe(II)	429 (113)		556 (13)	
Fe(II)CO	419 (188)	539 (14)		570 (16)

[a] pH 6.4 (Antonini & Brunori, 1971). [b] pH 7−10; this study.

Atomic coordinate errors for the His93Tyr variant were estimated by two methods. Examination of a plot of the crystallographic *R*-factor as a function of resolution yielded an estimate for the overall rms coordinate error for all atoms of 0.14 Å (Luzzati, 1952). On the basis of the Cruickshank (1949, 1954) method of evaluating individual atomic errors, the estimated overall rms coordinate error of the His93Tyr structure is 0.16 Å.

RESULTS

Electronic Spectroscopy. The absorption maxima and extinction coefficients of wild-type Mb and the His93Tyr variant are shown in Table 2. The spectra recorded for the wild-type protein are similar to those reported for sperm whale (Tamura et al., 1973; Egeberg et al., 1990) and human (Adachi et al., 1991, 1993) myoglobin. Notably, the Soret band of the Fe(III) derivative of the variant shifts from 408 nm (pH 6.4) observed for the wild-type protein to 403 nm. The extinction coefficient of the Soret band decreases from 188 mM^{-1} cm^{-1} for the wild-type protein to 111 mM^{-1} cm^{-1} for the variant. The electronic spectrum of the oxidized [Fe(III)] form of His93Tyr Mb is independent of pH between pH 7 and 10. Titration of His93Tyr with an excess of cyanogen bromide, which causes a blue shift and decrease in Soret intensity in wild-type myoglobin (Shiro & Morishima, 1984; Bracete et al., 1991; Adachi & Morishima, 1992), had no effect on the spectrum of the variant (data not shown). All of these observations suggest that the oxidized form of the variant possesses a five-coordinate Fe(III) center.

Thermal Denaturation. Thermal denaturation of the wild-type and variant proteins as monitored by circular dichroism spectroscopy is shown in Figure 1. The melting temperature (T_m) determined from the first derivative of the melting curve (Gwynneth et al., 1992) obtained by monitoring the ellipticity at 222 nm is ~75 °C for both the wild-type and variant proteins. Identical results were obtained by monitoring the ellipticity at the Soret band. Thus, replacement of the proximal histidine with a tyrosine causes no significant change in the thermostability of ferrimyoglobin.

Electrochemistry. The results of the photoreduction titrations of the His93Tyr variant are shown in Figure 2. Reduction of the variant shifts the Soret maximum from 403 nm observed for the oxidized protein to 429 nm. At pH 8.0

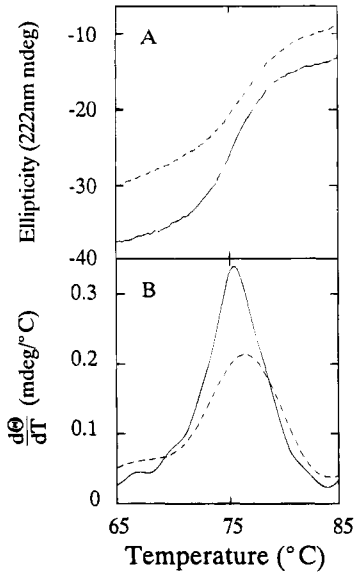

FIGURE 1: Thermal denaturation of wild-type (solid line) and His93Tyr (dashed line) horse heart myoglobin as determined by monitoring the change in ellipticity at 222 nm (A) and the corresponding first derivatives (B).

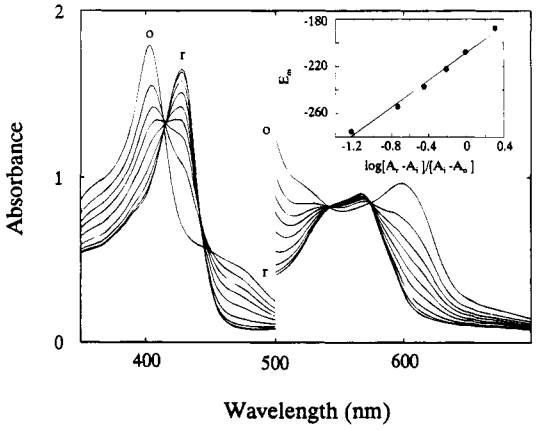

FIGURE 2: Spectroelectrochemical titration and corresponding Nernst plot (inset) of His93Tyr myoglobin (pH 8.0, 25 °C). Spectra of the completely oxidized (o) and completely reduced (r) species are labeled.

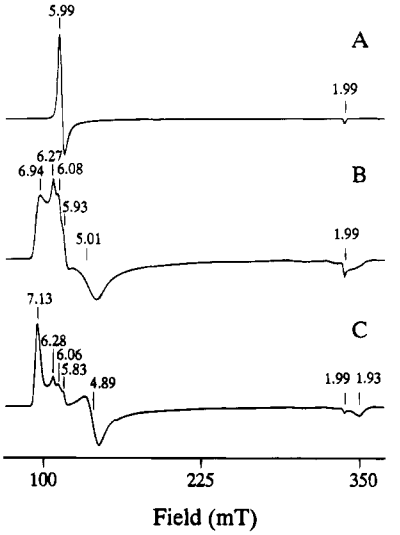

FIGURE 3: EPR spectra (4 K) of the high-spin ferric forms of (A) recombinant wild-type horse heart myoglobin (20 mM Tris-HCl/1 mM EDTA, pH 6.0), (B) the His93Tyr variant (20 mM Tris-HCl/1 mM EDTA, pH 8.0), and (C) the His93Tyr variant (sample B) diluted with an equal volume of 50% glycerol (initial [Mb] ~1 mM).

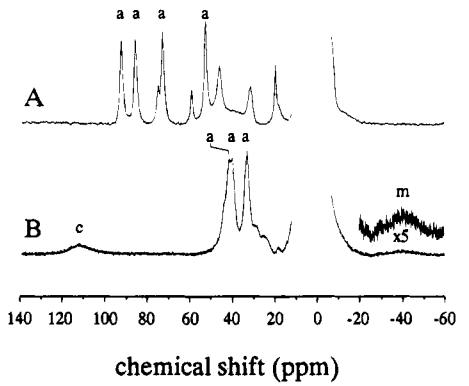

FIGURE 4: Hyperfine shifted region of the 200 MHz ^{1}H-NMR spectra of (A) recombinant wild-type horse heart metmyoglobin and (B) the His93Tyr variant in 50 mM deuterated sodium phosphate at pH 7.0 (uncorrected pH-meter reading) ([Mb] ~2 mM). The heme methyl (a) and *meso* (m) protons are labeled as are the *meta* protons (c) of the phenolate ligand.

(25 °C), the reduction potential of the His93Tyr variant is −208 mV (vs SHE). This value is substantially lower than that obtained for the wild-type protein [+45 mV vs SHE, pH 8.0 (Lim, 1990)] and is comparable to the value reported for the corresponding human Mb variant [−190 mV vs SHE (pH 7); Adachi et al., 1991]. This result is consistent with the presence of an anionic phenolate proximal ligand, which is expected to stabilize the Fe(III) form of the protein.

Electron Paramagnetic Resonance Spectroscopy. The EPR spectrum exhibited by the His93Tyr variant consists of a mixture of high-spin, rhombic components with *g* values of 6.94, 6.27, 6.08, 5.93, 5.01, and 1.99 (Figure 3). Addition of glycerol to the sample reduces protein heterogeneity (Bizzarri & Cannistraro, 1993) and resolves components with *g* values of 7.13, 6.28, 6.06, 5.83, 4.89, 1.99, and 1.93. The EPR spectrum of the His93Tyr variant is similar to that of bovine liver catalase which is also a high-spin, rhombic system (Williams-Smith & Patel, 1975; Blum et al., 1978; Palcic & Dunford, 1979). The EPR spectrum of bovine liver catalase, however, indicates the existence of pH-dependent forms (Blum et al., 1978), whereas the EPR spectrum of the variant is independent of pH between pH 7 and 10. The variant is unstable at pH <7, and no species resembling the hydroxo-bound (low-spin) form of wild-type ferrimyoglobin is observed at alkaline pH.

Nuclear Magnetic Resonance Spectroscopy. The heme substituents of the ferric His93Tyr variant in the absence of exogenous ligands exhibit much smaller chemical shifts than those of the wild-type protein in the low-field region of the ^{1}H-NMR spectrum (Figure 4). The spectrum of the His93Tyr variant is similar to the spectrum reported for the corresponding variant of human myoglobin (Adachi et al., 1993) and confirms the coordination of the phenolate group of Tyr93 to the heme iron. In the present case, however, a very broad resonance centered at −40 ppm not observed in the human variant can be identified that has been assigned to the *meso* protons of the macrocycle in model iron(III) porphyrin compounds (Arasasingham et al., 1990; Caughey & Johnson, 1969). The large upfield shift of this resonance is characteristic of five-coordinate high-spin Fe(III) (Bertini & Luchinat, 1986; Arasasingham et al., 1990; Rajarathnam et al., 1991). The broad signal at 112.5 ppm

arises from the two *meta* protons of the axially coordinated phenolate side chain. Similar chemical shifts have been observed for the *meta* protons of phenolate derivatives of high-spin ferric porphyrin compounds (Arasasingham et al., 1990; Garcia et al., 1991; Goff et al., 1984). In contrast to the present work, the two *meta* protons of the axial phenolate ligand in the His93Tyr variant of human myoglobin do not appear as a single resonance but exhibit different chemical shifts (Adachi et al., 1993).

X-ray Crystallography. The overall fold of the His93Tyr polypeptide chain is found to be similar to that of the wild-type protein except for the region around the mutation site and one of the associated helices (helix F) (Figure 5, top panel, and Figure 6a). The overall average positional difference between the two structures for main chain atoms is 0.42 Å. Significant deviations between main chain atoms in these two structures can be seen for residues 88−99 and 152−153. The latter two residues are substantially disordered and, therefore, poorly defined in both the wild-type and His93Tyr variant structures. As a result, the differences observed here probably reflect positional mobility in this region rather than a consequence of the mutation. The other region of significant backbone shift (residues 88−99) represents a displacement of the F helix away from the heme group. The difference matrix plot shown in Figure 5 (bottom panel) illustrates the impact of a tyrosine at position 93 on helix F in terms of both positional and thermal factor differences. Contours corresponding to differences in residues of the F helix are particularly prominent in this illustration. The average positional deviation of the main chain atoms in helix F is 1.33 Å, as compared to an average of 0.34 Å for all other main chain atoms in the polypeptide chain. Also, the average main chain thermal factors (Figure 5, bottom panel) are significantly greater for residues in the F helix of the variant (19.3 Å^2) than for the wild-type protein (13.6 Å^2). All other residues with significant average side chain positional deviations (>1.5 Å) are surface-exposed except for Leu29, which resides in the heme pocket.

A detailed comparison of the His93Tyr and wild-type structures near the mutation site is shown in Figure 6b. The hydroxyl group of Tyr93 occupies a position similar to that of the normally resident NE2 atom of His93 and is bound as the sixth ligand of the heme iron atom. However, the plane of the Tyr93 phenyl group is rotated by 71° relative to the plane of the imidazole ring present in the wild-type protein. The geometry of the ligand group approach to the heme also differs between these structures (Table 3), with the angle between the normal to the plane of the proximal ligand side chain and the normal to the porphyrin ring plane decreasing by ~31° in the Tyr93 variant. This appears to result from the need to accommodate the larger tyrosyl side chain in the heme pocket. The atoms of the Tyr93 side chain have an average thermal factor of 20.8 Å^2. This value is significantly greater than the corresponding value of 8.2 Å^2 observed for the His93 residue in wild-type myoglobin and indicates greater positional mobility in the side chain of Tyr93 relative to that of His93.

The orientation of the Tyr93 side chain is accompanied by several changes in heme geometry (see Table 3). If only the atomic positions of the atoms in the two heme structures are superimposed, the overall average difference is 0.56 Å. If all protein atoms are used in the least-squares fit to achieve heme overlap, the overall average positional difference of

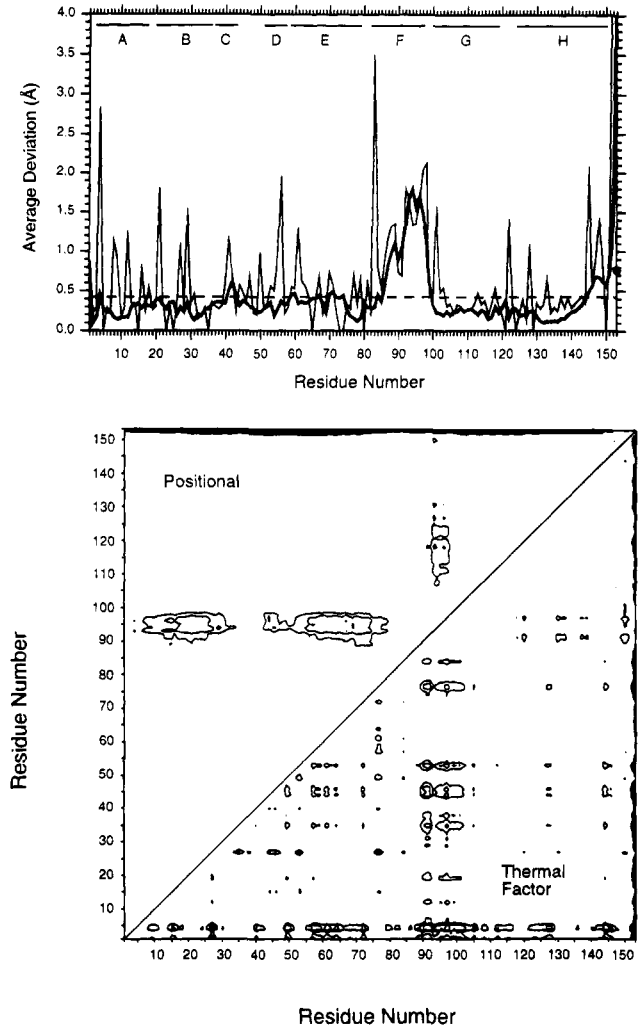

FIGURE 5: (Top panel) Average positional deviations observed in main chain (thick lines) and side chain (thin lines) atoms of the His93Tyr variant when compared to wild-type myoglobin. The horizontal dashed line indicates the average positional deviation (0.43 Å) for all main chain atoms. The filled circle at position 153 represents the average positional deviation of the atoms of the heme group. The alphabetical designation (A−H) of the helices in myoglobin is indicated at the top of this figure (Evans & Brayer, 1990). (Bottom panel) Positional and thermal factor difference matrix comparing the His93Tyr and wild-type myoglobin structures. The upper left half of the matrix contains the α-carbon distance differences, and the lower right half of the same matrix contains the average main chain thermal factor differences. Since both matrices are symmetrical about the diagonal, both may be combined in this way to eliminate redundancy. The value at a given point in the thermal factor difference matrix, $P_{x,y}$, represents an amino acid pairing (x,y) and was calculated with the equation $P_{x,y} = |(B_x - B_y)_{WT} - (B_x - B_y)_{His93Tyr}|$, where B is the average main chain thermal factor of a given amino acid residue. In the α-carbon distance difference section, the value at a point $P_{x,y}$ is calculated as $P_{x,y} = |(C_x - C_y)_{WT} - (C_x - C_y)_{His93Tyr}|$, where C is the α-carbon coordinate of a given residue. To identify significant differences, only those 1.7 standard deviations above the mean difference are contoured for both positional and thermal factor differences. Additional 1 standard deviation intervals are also contoured. Streaks in the matrix indicate sections of polypeptide chain with significant differences in either α-carbon positioning or average main chain thermal factor. For example, the region comprising residues 88−99 exhibits significant α-carbon distance differences, while residues 87−101 show significant average main chain thermal factor differences. An advantage of the difference matrix method of structural comparison is that it avoids potential bias from structural superposition and differences in overall thermal factor between the structures.

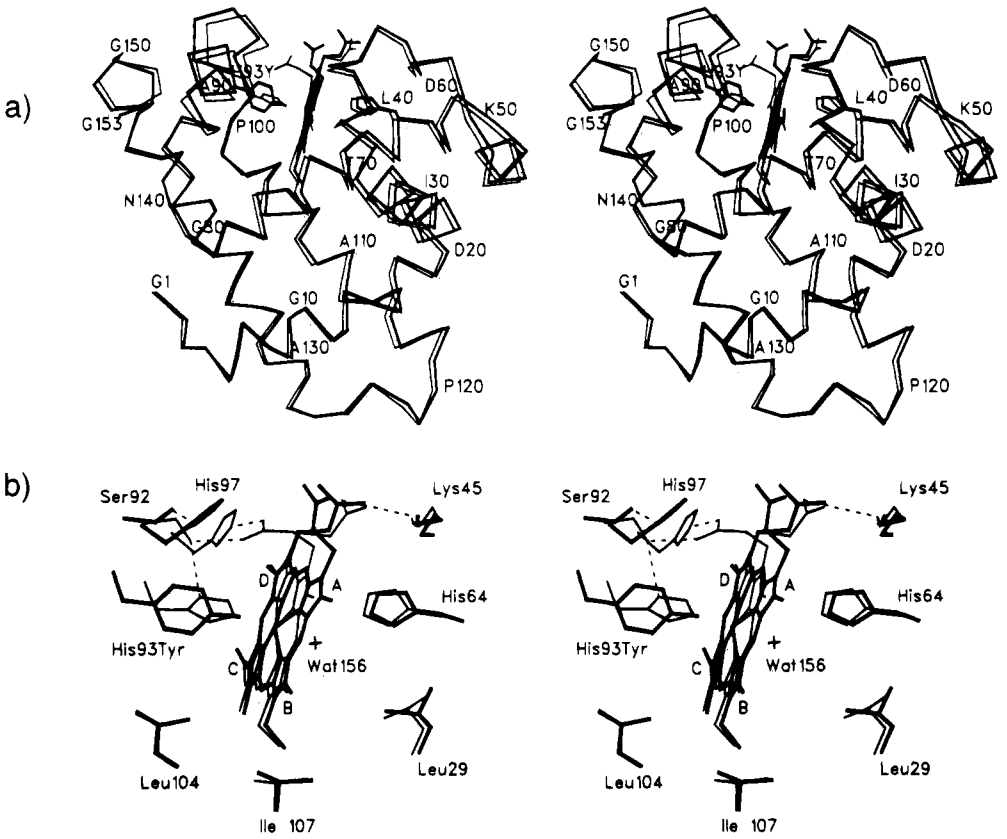

FIGURE 6: (a) Stereo drawing of the α-carbon backbones of the wild-type (thin lines) and His93Tyr variant (thick lines) myoglobin structures superimposed using a least-squares fit of main chain atoms. This diagram clearly shows the shift of residues 88−99 in helix F resulting from the substitution of a tyrosine residue for histidine 93. Also drawn are the side chains of residue 93 which in both proteins form a heme ligand interaction, the distal His64, and both heme groups. Every tenth residue has been labeled with its one-letter amino acid designation and its sequence number. For a complete listing of the sequence of horse heart myoglobin, see Evans and Brayer (1988). (b) Detailed stereo diagram showing the immediate environment of the mutation site. The structure of the His93Tyr variant is shown with thick lines, while the superimposed wild-type structure is represented with thin lines. The presence of Tyr93 causes significant positional shifts in the heme propionate groups, a vinyl group of the heme, and the side chains of Leu29, His64, Lys45, Ser92, and His97. Hydrogen bonds are indicated with dashed lines. Note that Wat156 is absent in the structure of the His93Tyr variant. The letter designations of each pyrrole ring of the heme are provided as a guide to discussion in the text.

all heme atoms is 0.77 Å. The heme iron atom has been drawn out of the plane of the porphyrin ring toward the hydroxyl group of Tyr93, with the distance between the iron atom and the porphyrin ring plane increasing from 0.12 Å in wild-type myoglobin to 0.45 Å in the His93Tyr structure. The displacement of heme iron toward Tyr93 may contribute to the loss of the distal water ligand (Wat156) in the His93Tyr structure. Notably, the vinyl group on pyrrole ring C in the variant has rotated 180°, so that it points in the direction of Lys42. The solvent accessibility of the heme (probe sphere radius of 1.4 Å; Connolly, 1983) is 154 Å^2, a value similar to that calculated (151 Å^2) for the wild-type structure.

The hydrogen bonding network around the heme is significantly altered in the His93Tyr variant (Figure 6b). Four hydrogen bonding interactions that are present in wild-type myoglobin are absent from the structure of the variant, while one new hydrogen bond is formed in the variant. On the pyroximal side of the heme, the hydrogen bonds normally formed by the Ser92 hydroxyl to the ND1 atom of His93 and the O2A carboxyl oxygen of propionate A are lost. As a consequence, the hydroxyl group of Ser92 rotates toward the side chain of His97 and forms a new hydrogen bond with the ND1 atom of that residue. This interaction is made possible by a 160° rotation about the $C_\alpha-C_\beta$ bond of the His97 side chain in the variant. The hydrogen bond normally formed by the NE2 atom of His97 with the carboxyl group of propionate A (O1A oxygen atom) is not observed in the His93Tyr variant owing to the increased distance between these two groups that results from the overall displacement of helix F (Figure 6b) as well as the subsequent reorientation of the side chain of His97. Coincident with the loss of its interactions with Ser92 and His97, propionate A rotates toward the surface of the protein where it interacts with bulk solvent.

Significant changes also occur on the distal side of the heme (Figure 6b). The distal heme iron water ligand (Wat156) found in the wild-type protein is not observed in the His93Tyr structure. This water molecule normally forms a hydrogen bond to His64, the side chain of which shifts by 0.43 Å in the variant to form a weak interaction (3.7 Å) with the side chain of Lys45. The side chain of the adjacent residue Leu29 is also reoriented, presumably in response to the movement of His64. Hydrogen bonding interactions of the propionate group on pyrrole ring D are also altered in the variant. In wild-type myoglobin, this propionate forms hydrogen bonds with the NZ atom of Lys45 and two water molecules. In the His93Tyr structure, a shift of the Lys45 side chain away from the heme toward His64 results in the loss of the hydrogen bond formed between Lys45 and propionate D. In wild-type myoglobin, the side chain of Lys45 also forms hydrogen bonds to two water molecules.

Table 3: Heme Geometry of Wild-Type and His93Tyr Mutant Myoglobins[a]

protein	wild-type	His93Tyr
(I) Angular Deviations (deg) of Pyrrole Ring Plane Normals and Heme Coordinate Bonds from the Porphyrin Ring Plane Normal		
A	4.01	4.93
B	4.09	1.74
C	4.10	8.62
D	3.61	2.87
Fe-His93 NE2	1.15	
Fe-Tyr93 OH		7.22
(II) Angular Deviations (deg) of the Pyrrole Ring Plane Normals from Pyrrole Nitrogen Plane Normal		
A	5.57	2.33
B	4.72	4.20
C	7.39	11.46
D	6.37	1.79
(III) Angular Deviation (deg) of the Ring Plane Normal of the Proximal Ligand Side Chain from the Porphyrin Ring Plane Normal		
His 93	89.7	
Tyr93		58.2
(IV) Heme Iron Ligand Bond Distances (Å)		
His93 NE2	2.25	
Tyr93 OH		1.91
Wat156 O	2.27	
Hem-NA	2.16	2.06
Hem-NB	1.94	1.99
Hem-NC	2.14	2.06
Hem-ND	1.99	2.01

[a] The pyrrole nitrogen plane is defined by the four pyrrole nitrogens of the heme group. The four pyrrole ring planes are each defined by the five atoms of the ring and the first carbon atom attached to each of the four carbons of the ring. The porphyrin ring is defined by the 5 atoms in each of the 4 pyrrole rings, the 4 bridging methine carbon atoms, the first carbon atom of each of the 8 side chains of the heme, and the central iron atom of the heme (33 atoms in total). The plane of the histidine side chain is defined by the five atoms in the imidazole ring. The plane of the tyrosine side chain is defined by the six carbon atoms of the phenyl ring and the hydroxyl oxygen atom. The heme atom nomenclature used in this table follows the conventions of the Protein Data Bank (Bernstein et al., 1977) and is diagrammatically illustrated in Figure 3 of Berghuis and Brayer (1992).

These interactions are replaced in the His93Tyr structure by a single hydrogen bond to a well-defined water molecule.

DISCUSSION

Replacement of the proximal His ligand of myoglobin with a tyrosyl residue produces a variety of interrelated functional and structural changes to the protein that provide insight into the fundamental role that the proximal ligand plays in dictating the properties of heme proteins in general. Interestingly, although the tyrosyl side chain is larger than that of a histidyl residue, the heme binding site can adjust to accommodate the new residue through displacement and increased mobility for the F helix, without a concomitant decrease in overall thermal stability. Moreover, NMR, electronic, and EPR spectroscopy as well as the crystallographically determined three-dimensional structure all indicate that in contrast to the wild-type protein, the ferric form of the variant is five-coordinate under all conditions considered in this study.

The NMR spectra obtained in the current study differ from those reported previously for the corresponding His93Tyr variant of human myoglobin (Adachi et al., 1993) in that the two *meta* protons of the proximal phenolate exhibit different chemical shifts (128.1 and 107 ppm) in the human protein. In contrast, the spectrum of the His93Tyr variant of the horse heart protein studied here exhibits a single signal at 112 ppm that is attributable to these protons. For the phenolate ligands of Fe(III) protoporphyrin IX model compounds in which there are no steric constraints on the orientation of the axial ligand relative to the porphyrin ring, the two *meta* protons of the phenolate ligand exhibit the same chemical shift (Caughey & Johnson, 1969; Arasasingham et al., 1990). In related systems where the phenolate ligand is held in a restricted rotation, the two *meta* protons exhibit different chemical shifts (Goff et al., 1984). With pendant-capped Fe(III) porphyrins in which the axial phenolate is forced into a fixed conformation and the porphyrin ring is perfectly symmetric, these protons exhibit identical chemical shifts because their chemical environments are the same (Garcia et al., 1991). On the basis of these reports for model compounds, the current result indicates that the environments of these protons are equivalent in the horse heart protein and, therefore, implies that the phenolate ring of the bound Tyr residue can flip at a rate that is fast on the time scale of the NMR measurement.

A more specific mechanistic origin for this observation can be derived by a detailed comparison of the horse heart and human myoglobin structures. The amino acid sequences of horse heart and human myoglobin differ at 17 positions. Examination of the three-dimensional structure of the horse heart protein reveals that the side chain of Ile142 is the only one of these groups that is located in proximity to the proximal ligand to the heme iron. Although the three-dimensional structures of human myoglobin and its His93Tyr variant are not currently available, we estimate that the closest approach of the Ile142 side chain to the Tyr93 side chain in the variant is ~0.7−1.0 Å greater than the shortest distance between the nearest atom of Met142 in the corresponding human variant. We, therefore, suggest that the Met142 residue in the human protein constrains the rotation of the proximal Tyr ligand to the heme iron in the His93Tyr variant of human myoglobin.

The mechanism by which a tyrosyl residue is accommodated to provide a stable environment for heme binding is apparent from the three-dimensional structure of the variant determined by X-ray diffraction analysis. The principal conformational change observed in the structure of this variant is the displacement of the F helix, in which the proximal His ligand resides, away from the heme (Figure 6). This movement of the F helix is accompanied by a shift of the heme iron atom out of the plane of the porphyrin ring toward Tyr93 and by an increase in the thermal factors of the residues in this helix that is indicative of increased conformational flexibility in the variant. It is also notable that the average side chain thermal factor for Tyr93 in the variant is 20.8 Å^2 compared to 8.2 Å^2 for the normally resident His93. At the same time, the water molecule bound as the sixth ligand in wild-type myoglobin is lost, and the side chain of Tyr93 rotates relative to the position of the His93 imidazole group so that the angle between the plane of the residue 93 side chain and the porphyrin ring decreases. The positions of the heme substituents remain unaffected by the mutation, except for rotation of the vinyl group of pyrrole ring C toward Lys42 and rotation of the A propionate group to a more solvent-exposed location (Figure 6).

The positional changes caused by the mutation are accompanied by five changes in hydrogen bonding interactions that involve either substituents of the heme prosthetic group or residues that are in the heme binding pocket. Ser92 is involved in three of these five changes in that the hydrogen bonds normally formed by Ser92 with the propionate A and with His93 are not present in the variant, while a new hydrogen bond is formed between the Ser92 OH group and the ND1 atom of His97. In addition, the hydrogen bond between the His97 NE2 atom and propionate A and the hydrogen bond formed by Lys45 and propionate D are not present in the variant. The loss of three hydrogen bonds formed by heme substituents in the wild-type protein probably contributes to the increased thermal factors observed for atoms of the F helix and may explain the decreased stability of the variant at pH <7. It is also conceivable that the reduced number of interactions between the heme prosthetic group and the apoprotein may contribute to the expression of this variant in *E. coli* as the apoprotein rather than as the holoprotein as observed for the wild-type protein. Nevertheless, at neutral or alkaline pH, the stability of the reconstituted Fe(III) protein appears to be comparable to that of the wild-type protein (Figure 1).

The movement of the F helix away from the heme prosthetic group draws the heme iron atom out of the plane of the heme toward the Tyr93 ligand. Similar displacement of the heme iron has been observed for five-coordinate model heme complexes (Koenig, 1965; Hoard et al., 1965). The position of the Tyr93 residue relative to the heme group resembles that of bovine liver catalase. In both proteins, the plane of the tyrosine ring eclipses the Fe−pyrrole nitrogen bonds of pyrroles B and D. However, the tyrosine ligand in bovine catalase forms a hydrogen bond with an adjacent arginine side chain that is analogous to the hydrogen bond formed by the Ser92 OH group and the proximal His residue of wild-type protein. No hydrogen bonding interactions of this type occur in the His93Tyr variant.

The movement of the F helix combined with the greater electronegativity of the tyrosyl oxygen atom (relative to His) presumably reduces the affinity of the iron for coordination of water as the sixth ligand. Interestingly, the three-dimensional structures of the bovine liver (Reid et al., 1981; Murthy et al., 1981; Fita & Rossman, 1985, 1986) and fungal catalases (Vainshtein et al., 1986) indicate that the sixth coordination positions of these proteins are also unoccupied while similar studies indicate that a water molecule is bound as the sixth heme iron ligand in the bacterial catalase (Murshudov et al., 1992). From this limited number of structures, it appears that although the presence of a proximal tyrosyl ligand increases the probability of a pentacoordinated heme iron, other structural factors may overcome this propensity.[1]

Intriguing functional considerations regarding this variant include its reactions with dioxygen and with hydrogen peroxide. We attempted to prepare the oxyMb derivative of this variant by reduction of the metMb derivative with dithionite followed quickly by elution over a column of Sephadex G-25 that had been washed with argon-purged buffer. While this method is sufficient for generation of wild-type oxyMb, the variant rapidly autoxidized, presumably owing to its low reduction potential (data not shown). Related behavior was noted previously for other species of this variant (Adachi et al., 1991, 1993; Egeberg et al., 1990a,b). Thus, characterization of the oxygen binding properties of this variant is not feasible. Similar to previous observations with the corresponding variant of human Mb (Adachi et al., 1993), addition of a 10-fold excess of hydrogen peroxide to the His93Tyr metMb derivative results in a prompt decrease in the intensity of the Soret band that is indicative of heme degradation with no evidence for transient formation of the ferryl derivative that such treatment produces for wild-type myoglobin (e.g., Wittenberg, 1978). Similarly, the peroxidase activity of the variant measured with ABTS as an electron donor (pH 7, 25 °C) was about 30-fold lower than that of the wild-type proteins (data not shown). As Adachi et al. (1993) have reported catalase activities for this variant of the human protein that are about one-third the activity of wild-type myoglobin, it seems clear that replacement of the proximal His ligand of myoglobin with a Tyr residue is not sufficient to convert Mb to an effective enzyme. This finding is not surprising in light of the many additional structural differences that distinguish peroxidases, catalases, and myoglobin from each other.

The altered hydrogen bonding interactions of the heme substituents and Ser92 observed here illustrate the subtle structural changes that can result from modification of critical active site residues in proteins of this type. Similarly, comparison of the current NMR results with those obtained for the corresponding variant of human myoglobin demonstrates the subtle manner in which apparently small species-dependent structural differences can produce significant effects on the dynamics of protein structure.

[1] A low-resolution study of Hb Iwate in which the proximal His of the α-chain is replaced by a Tyr residue suggests that this variant may be six-coordinate with the iron binding both to the distal His residue and the proximal Tyr residue (Greer, 1971).

ACKNOWLEDGMENT

We thank Nham Nguyen for skilled technical assistance in the preparation of protein crystals and Dr. Yaoguang Luo for assistance with the R-AXIS II area detector system.

REFERENCES

Adachi, S., & Morishima, I. (1992) *Biochemistry 31*, 8613−8618.

Adachi, S., Nagano, S., Watanabe, Y., Ishimori, K., & Morishima, I. (1991) *Biochem. Biophys. Res. Commun. 180*, 138−144.

Adachi, S., Sunohara, N., Ishimori, K., & Morishima, I. (1992) *J. Biol. Chem. 267*, 12614−12621.

Adachi, S., Nagano, S., Ishimori, K., Watanabe, Y., Morishima, I., Egawa, T., Kitigawa, T., & Makino, R. (1993) *Biochemistry 32*, 241−252.

Antonini, E., & Brunori, M. (1971) *Hemoglobin and Myoglobin in their Reactions with Ligands*, North-Holland Publishing Co., Amsterdam, The Netherlands.

Arasasingham, R. D., Balch, A. L., Cornman, C. R., de Ropp, J. S., Eguchi, K., & La Mar, G. N. (1990) *Inorg. Chem. 29*, 1847−1850.

Berghuis, A. M., & Brayer, G. D. (1992) *J. Mol. Biol. 223*, 959−976.

Bernstein, F. C., Koetzle, T. F., Williams, G. J. B., Meyer, E. F., Jr., Brice, M. D., Rodgers, J. R., Kennard, O., Shimanouchi, T., & Tasumi, M. (1977) *J. Mol. Biol. 112*, 535−542.

Bertini, I., & Luchinat, C. (1986) in *NMR of Paramagnetic Molecules in Biological Systems*, pp 165−229, Benjamin Cummings, Menlo Park, CA.

Bizzarri, A. R., & Cannistraro, S. (1993) *Eur. Biophys. J. 22*, 259−267.

Blum, H., Chance, B., & Litchfield, W. J. (1978) *Biochim. Biophys. Acta 534*, 317−321.
Bracete, A. M., Sono, M., & Dawson, J. H. (1991) *Biochim. Biophys. Acta 1080*, 264−270.
Brünger, A. T. (1990) X-PLOR, version 2.1, Yale University Press, New Haven, CT.
Caughey, W. S., & Johnson, L. F. (1969) *J. Chem. Soc., Chem. Commun.*, 1362−1363.
Connolly, M. L. (1983) *Science 221*, 709−713.
Cruickshank, D. W. J. (1949) *Acta Crystallogr. 2*, 65−82.
Cruickshank, D. W. J. (1954) *Acta Crystallogr. 7*, 519.
De Duve, C. (1948) *Acta Chem. Scand. 2*, 264.
Draper, R. D., & Ingraham, L. L. (1968) *Arch. Biochem. Biophys. 125*, 802−808.
Egeberg, K. D., Springer, B. A., Martinis, S. A., Sligar, S. G., Morikis, D., & Champion, P. M. (1990) *Biochemistry 29*, 9783−9791.
Evans, S. V., & Brayer, G. D. (1988) *J. Biol. Chem. 263*, 4263−4268.
Evans, S. V., & Brayer, G. D. (1990) *J. Mol. Biol. 213*, 885−897.
Fita, I., & Rossmann, M. G. (1985) *J. Mol. Biol. 185*, 21−37.
Fita, I., & Rossmann, M. G. (1986) *Acta Crystallogr. B42*, 497−503.
Garcia, B., Lee, C., Blasko, A., & Bruice, T. C. (1991) *J. Am. Chem. Soc. 113*, 8118−8126.
Goff, H. M., Shimomura, E. T., Lee, Y. J., & Scheidt, W. R. (1984) *Inorg. Chem. 23*, 315−321.
Greer, J. (1971) *J. Mol. Biol. 59*, 67−126.
Guillemette, G., Matsushima-Hibiya, Y., Atkinson, T., & Smith, M. (1991) *Protein Eng. 4*, 585−592.
Gwynneth, M. E., Huber, H. E., DeFeo-Jones, D., Vuocolo, G., Goodhart, P. J., Maigetter, G. S., Oliff, A., & Heimbrook, D. C. (1992) *J. Biol. Chem. 267*, 7971−7974.
Hargrove, M. S., Singleton, E. W., Quillen, M. L., Ortiz, L. A., Phillips, G. N., Olson, J. S., & Mathews, A. J. (1994) *J. Biol. Chem. 269*, 4207−4214.
Hendrickson, W. A., & Konnert, J. (1981) in *Biomolecular Structure, Function, Conformation and Evolution* (Srinivasan, R., Ed.) Vol. 1, pp 43−57, Pergamon Press, Oxford.
Hoard, J. L., Hamor, M. J., Hamor, T. A., & Caughey, W. S. (1965) *J. Am. Chem. Soc. 87*, 2312−2319.
Inubushi, T., & Becker, E. D. (1983) *J. Magn. Reson. 51*, 128−133.
Koenig, D. F. (1965) *Acta Crystallogr. 18*, 663.
Leung, C. J., Nall, B. T., & Brayer, G. D. (1989) *J. Mol. Biol. 206*, 783−785.
Lim, A. R. (1990) Ph.D. Dissertation, University of British Columbia, Vancouver.
Lloyd, E., & Mauk, A. G. (1994) *FEBS Lett. 340*, 281−286.
Luzzati, V. (1952) *Acta Crystallogr. 5*, 802−810.
Maniatis, T., Fritsch, E. F., & Sambrook, J. (1989) *Molecular Cloning: A Laboratory Manual*, Cold Spring Harbor Laboratory Press, Cold Spring Harbor, NY.
Mauro, J. M., Fishel, L. A., Hazzad, J. T., Meyer, T. E., Tollin, G., Cusanovich, M. A., & Kraut, J. (1988) *Biochemistry 27*, 6243−6256.
Maurus, R., Bogumil, R., Luo, Y., Tang, H.-L., Smith, M., Mauk, A. G., & Brayer, G. D. (1994) *J. Biol. Chem. 259*, 12606−12610.
Morikis, D., Champion, P. M., Springer, B. A., & Sligar, S. G. (1989) *Biochemistry 28*, 4791−4800.
Murshudov, G. N., Melik-Adamyan, W. R., Grebenko, A. I., Barynin, V. V., Vagin, A. A., Vainshtein, B. K., Dauter, Z., & Wilson, K. S. (1992) *FEBS Lett. 312*, 127−131.
Murthy, M. R., Reid, T. J., III, Sicignano, A., Tanaka, N., & Rossman, M. G. (1981) *J. Mol. Biol. 152*, 465−499.
Palcic, M., & Dunford, H. B. (1979) *Can. J. Biochem. 57*, 321−329.
Quillin, M. L., Arduini, R. M., Olson, J. S., & Phillips, G. N. (1993) *J. Mol. Biol. 234*, 140−155.
Rajarathnam, K., La Mar, G. N., Chiu, M. L., Sligar, S. G., Singh, J. P., & Smith, K. (1991) *J. Am. Chem. Soc. 113*, 7886−7892.
Reid, T. J., III, Murthy, M. R. N., Sicignano, A., Tanaka, N., Musick, W. D. L., & Rossmann, M. G. (1981) *Proc. Natl. Acad. Sci. U.S.A. 78*, 4767−4771.
Rizzi, M., Bolognesi, M., Coda, A., Cutruzzola, F., Allocatelli, C., Brancaccio, A., & Brunori, M. (1993) *FEBS Lett. 320*, 13−16.
Sato, M., Yamamoto, M., Imada, K., Katsube, Y., Tanaka, N., & Higashi, T. (1992) *J. Appl. Crystallogr. 25*, 348−357.
Shiro, Y., & Morishima, I. (1984) *Biochemistry 23*, 4879−4884.
Springer, B. A., Sligar, S. G., Olson, J. S., & Phillips, G. N., Jr. (1994) *Chem. Rev. 94*, 699−714.
Tamura, M., Asakura, T., & Yonetani, T. (1973) *Biochim. Biophys. Acta 295*, 467−479.
Tong, H., Berghuis, A. M., Chen, J., Luo, Y., Guss, J. M., Freeman, H. C., & Brayer, G. D. (1994) *J. Appl. Crystallogr. 27*, 421−426.
Vainshtein, B. K., Melik-Adamyan, W. R., Barynin, V. V., Vagin, A. A., Grebenko, A. I., Borisov, V. V., Bartels, K. S., Fita, I., & Rossmann, M. G. (1986) *J. Mol. Biol. 188*, 49−61.
Williams-Smith, D. L., & Patel, K. (1975) *Biochim. Biophys. Acta 405*, 243−252.
Wittenberg, J. B. (1978) *J. Biol. Chem. 253*, 5694−5695.
Zoller, M. J., & Smith, M. (1983) *Methods Enzymol. 100*, 468−500.
Zoller, M. J., & Smith, M. (1984) *DNA 3*, 479−488.

BI941953A